53rd AIAA/ASME/ASCE/AHS/ASC Structures, Structural Dynamics and Materials Conference
20th AI
23 - 26 April 2012, Honolulu, Hawaii

AIAA 2012-1457

Extension-Twist coupled laminates for aero-elastic compliant blade design.

C. B. York*
University of Glasgow, Glasgow, Scotland, G12 8QQ

A definite list of laminate configurations with extension-twisting (and shearing-bending) coupling is derived for up to 21 plies of identical thickness. The list comprises individual stacking sequences, containing standard angle-ply and cross-ply sub-sequences; combinations which are contrary to the previously assumed form for this class of laminate. The list also contains dimensionless parameters from which the extensional, coupling and bending stiffness terms are readily calculated for any fiber/matrix system. Lamination parameters are shown graphically to illustrate the extent of the design space with up to 21 plies. A special sub-group from this class of coupled laminate is identified that can be manufactured flat under a standard elevated temperature curing process; this sub-group possesses hygro-thermally curvature-stable behavior. Finally, bounds on the compression buckling strength are assessed using a closed form solution for all the laminate groups presented.

Nomenclature

$\mathbf{A}$,A_{ij}	=	extensional (membrane) stiffness matrix and its elements (i,j = 1, 2, 6).
$\mathbf{B}$,B_{ij}	=	bending-extension-coupling stiffness matrix and its elements (i,j = 1, 2, 6).
$\mathbf{D}$,D_{ij}	=	bending (flexural) stiffness matrix and its elements (i,j = 1, 2, 6).
H	=	laminate thickness (= $n \times t$).
n	=	number of plies in laminate stacking sequence.
$\mathbf{N}$	=	in-plane force resultants (= $\{N_x,N_y,N_{xy}\}^T$).
N_x,N_y	=	in-plane axial load per unit length.
N_{xy}	=	in-plane shear flow.
$\mathbf{M}$	=	out-of-plane moment resultants (= $\{M_x,M_y,M_{xy}\}^T$).
M_x,M_y	=	bending moments per unit length about principal axes.
M_{xy}	=	twist moment per unit length.
Q_{ij}	=	reduced stiffness (i,j = 1, 2, 6).
Q'_{ij}	=	transformed reduced stiffness (i,j = 1, 2, 6).
t	=	ply thickness.
x,y,z	=	principal axes.
α_{Iso},α_1,α_2		thermal expansion coefficients
β		off-axis alignment angle of principal fibre direction
$\boldsymbol{\varepsilon}$	=	in-plane strains (= $\{\varepsilon_x,\varepsilon_y,\gamma_{xy}\}^T$).
ε_x,ε_y	=	in-plane axial strains.
γ_{xy}	=	in-plane shear strain.
$\boldsymbol{\kappa}$	=	Curvatures (= $\{\kappa_x,\kappa_y,\kappa_{xy}\}^T$).
κ_x,κ_y	=	curvatures about principal axes.
κ_{xy}	=	twist curvature.
$\xi_{1\text{-}4}$	=	lamination parameters for extensional stiffness ($\xi_1,\xi_2,\xi_3,\xi_4 = \xi_1^A,\xi_2^A,\xi_3^A,\xi_4^A$).
$\xi_{5\text{-}8}$	=	lamination parameters for coupling stiffness ($\xi_5,\xi_6,\xi_7,\xi_8 = \xi_1^B,\xi_2^B,\xi_3^B,\xi_4^B$).
$\xi_{9\text{-}12}$	=	lamination parameters for bending stiffness ($\xi_9,\xi_{10},\xi_{11},\xi_{12} = \xi_1^D,\xi_2^D,\xi_3^D,\xi_4^D$).
χ,$\chi_{\pm}$,$\chi_{\cap}$,$\chi_{\bullet}$	=	coupling stiffness parameter for laminate, and angle-ply and cross-ply sub-sequences.

* Senior Lecturer, School of Engineering.

$\zeta,\zeta_{\pm},\zeta_{\cap},\zeta_{\blacktriangle}$ = bending stiffness parameter for laminate, and angle-ply and cross-ply sub-sequences.
$+,-,\pm$ = angle plies, used in stacking sequence definition.
$\mathrm{O},\bullet$ = cross plies, used in stacking sequence definition.

Keywords

Coupled Laminates, Lamination Parameter Design Space, Extension-Twisting, Hygro-Thermally Curvature-Stable Lamination Parameters, Quasi-Homogeneous, Shearing-Bending, Angle-Ply Laminates, Standard-Ply Laminates.

I. Introduction

This article is one of a series addressing a unified approach to the characterization of coupled composite laminates, which includes all possible interactions between extension, shearing, bending and twisting. These complex mechanical couplings are not present in conventional materials, such as metals, and therefore represent an important and significant enabling technology. However, many coupled laminate designs lead to undesirable warping distortions as a result of the high temperature curing process, and sophisticated tailoring methods are necessary to design configurations that are immune to such effects. One family of coupled laminate, with immunity to thermal warping[1-3], has been used extensively for application to tilt-rotor blade design. Here, extension-twisting coupling, at the structural or blade level, is used to develop optimized twist distribution along the blade for both hover and forward flight: a change in rotor speed, and the resulting centrifugal forces, provides the required twist differential between the two flight regimes. This behavior is achieved from laminate level extension-shearing coupling, through off-axis alignment of a balanced and symmetric laminate. However, such laminate designs possess significant bending-twisting coupling at the laminate level, leading to detrimental effects on the compression buckling strength of the blade; which represents an important static design constraint.

Extension-shearing coupled laminates have also been employed[4] to achieve bending-twisting behavior at the wing-box level; achieved this time through un-balanced, symmetric laminates rather than through off-axis alignment of the principal material axis of balanced and symmetric laminates. Bending-twisting coupling at the laminate level is again present in such designs. A definitive list of unbalanced, extension-shearing coupled laminates with standard ply orientations has since been derived[5], demonstrating that compression buckling strength can be substantially improved in the absence of laminate level bending-twisting coupling without affecting the bending-twisting response at the structural or wing-box level. Similar laminate design concepts are now applied to the design of wind-turbine blades to induce bending-twisting coupling for passive load-alleviation[6].

By contrast to the preceding laminate class, a unique sub-class of laminate with extension-twisting coupling was shown[2,7] to be immune to the severe thermal warping distortions affecting the vast majority of configurations with this form of mechanical coupling; which require specially curved tooling in order to possess the required shape after high temperature curing. This hygro-thermally curvature-stable or warp-free laminate sub-class also facilitates the design of aero-elastic compliant rotor blades with extension-twisting coupling; this time by employing extension-twisting coupling rather than extension-shearing coupling at the laminate level. The discovery of this particular class of coupled laminate has had a strong influence on the subsequent studies in the literature, including: maximizing the extension-twisting coupling response[8,9] and/or; integrating additional forms of mechanical coupling response, e.g. bending-twisting coupling[10].

II. Characterization of laminated composite materials

Composite laminates are typically characterized in terms of their response to mechanical (and/or thermal) loading, which is generally associated with a description of the coupling behavior, unique to this type of material. The well-known **ABD** relation from classical lamination theory is often expressed using compact notation:

$$\begin{Bmatrix} \mathbf{N} \\ \mathbf{M} \end{Bmatrix} = \begin{bmatrix} \mathbf{A} & \mathbf{B} \\ \mathbf{B} & \mathbf{D} \end{bmatrix} \begin{Bmatrix} \boldsymbol{\varepsilon} \\ \boldsymbol{\kappa} \end{Bmatrix} \tag{1}$$

The coupling behavior, which is dependent on the form of the elements in each of the extensional (**A**), coupling (**B**) and bending (**D**) stiffness matrices, is conveniently described by an extended subscript notation, defined previously in an Engineering Sciences Data Unit, or ESDU data item[11]. Here, a balanced and symmetric stacking sequence, which generally give rise to coupling between bending and twisting[13] and are referred to by the designation $\mathbf{A}_S\mathbf{B}_0\mathbf{D}_F$, signifying that the elements of the extensional stiffness matrix ($\mathbf{A}_S$) have the specially

orthotropic or simple form:

$$\begin{bmatrix} A_{11} & A_{12} & 0 \\ & A_{22} & 0 \\ \text{Sym.} & & A_{66} \end{bmatrix} \tag{2}$$

the bending-extension coupling matrix ($\mathbf{B}_0$) is null, i.e. no coupling between in-plane and out-of-plane responses, whilst all elements of the bending stiffness matrix ($\mathbf{D}_F$) are Finite, and have the form:

$$\begin{bmatrix} D_{11} & D_{12} & D_{16} \\ & D_{22} & D_{26} \\ \text{Sym.} & & D_{66} \end{bmatrix} \tag{3}$$

It is now well understood that the extensional (**A**) and bending (**D**) stiffness matrices possess one of two forms: either fully uncoupled ($\mathbf{A}_S$, $\mathbf{D}_S$) or fully coupled ($\mathbf{A}_F$, $\mathbf{D}_F$). The isotropic form of these matrices, where $\mathbf{D}_I$ and/or $\mathbf{A}_I$ replace $\mathbf{D}_S$ and/or $\mathbf{A}_S$ respectively, have been shown to represent subsets of the specially orthotropic (uncoupled or simple) form[12].

An additional subset includes laminates for which the elements of the bending stiffness matrix are related directly to those of the extensional stiffness matrix by:

$$D_{ij} = A_{ij}H^2/12 \tag{4}$$

with respect to the laminate thickness, H. This subset represents a significant simplification in design, and for the uncoupled form ($\mathbf{A}_S$, $\mathbf{D}_S$) can be described as a Quasi-Homogeneous Orthotropic Laminate, or **QHOL**, providing concomitant properties in both extension and bending, thus providing maximum (and minimum) in-plane and out-of-plane reinforcement in the same direction.

In contrast to the uncoupled or simple form of the extensional ($\mathbf{A}_S$) and bending ($\mathbf{D}_S$) stiffness matrices, the coupling (**B**) stiffness matrix has several complex forms: $\mathbf{B}_0$ in the preceding laminate descriptions must now be replaced with one of the alternative designations given in Table 1, giving rise to twenty-four possible combinations, presented elsewhere[14].

The laminates investigated in this study are free from coupling between the shear force resultant (N_{xy}) and extensional strains (ε_x, ε_y), i.e. $A_{16} = A_{26} = 0$, and free from coupling between moment resultants (M_x, M_y) and twist curvature (κ_{xy}), i.e. $D_{16} = D_{26} = 0$. However, they possess coupling between extension and twisting and between shearing and bending, i.e. in-plane force resultants (N_x and N_y) give rise to twist curvature (κ_{xy}) and a shear force resultant (N_{xy}) gives rise to bending curvatures (κ_x and κ_y).

Fully uncoupled laminates minimize distortion during manufacturing and generally maximize compression buckling strength, particularly in comparison to balanced and symmetric laminate configurations described above, which are commonly adopted in aircraft and spacecraft construction, despite the fact that such laminates possess bending anisotropy, i.e. coupling between bending and twisting. Ignoring such coupling responses continues to be justified on the basis that the effects dissipate for laminates with a large number of plies when heuristic design rules are applied, e.g., applying a constraint on the maximum number of contiguous plies of identical orientation. However the response may be strongly coupled in thin laminates.

Coupled laminates are often subject to thermal distortions due to the high temperature curing process requirement for high strength fiber/matrix systems. However, continuing developments in matrix technologies may render such requirements unnecessary in future; at which point the entire design space of laminate configurations identified in this article may be readily exploited. Current design of coupled laminates is therefore constrained by either manufacturing technology, in which tooling must be shaped in order to mitigate the thermal distortions on cooling, or to stacking sequence configurations which exhibit hygro-thermally curvature-stable response; the latter is considered in this article.

In order characterize the thermal and/or mechanical coupling behavior, a response-based labeling is presented alongside and complementary to the subscript notation in Table 1. The subscripts for the coupling (**B**) matrix in Table 1 follow exactly the same logic as described for the Extensional (**A**) and Bending (**D**) matrices. The complexities of the **B** matrix are in fact captured by only two additional subscripts. Subscript *l* denotes that the

*l*eading diagonal elements (B_{11}, $B_{22} \neq 0$) are non-zero, whereas subscript *t* denotes that off-diagonal (or *transverse*) elements (B_{16}, $B_{26} \neq 0$) are non-zero. These two cases may also be superimposed.

Table 1 – Compact notation, coupling behavior using response-based labeling and associated form of coupling stiffness matrix. Subscripts associated with compact notation, after ESDU[11], are summarized in the table footnotes.

Compact notation	Response-based labeling	Matrix form
$\mathbf{B}_l$	Extension-Bending; *E-B*	$\begin{bmatrix} B_{11} & 0 & 0 \\ 0 & B_{22} & 0 \\ 0 & 0 & 0 \end{bmatrix}$
$\mathbf{B}_t$	Extension-Twisting and Shearing-Bending; *E-T*-*S-B*	$\begin{bmatrix} 0 & 0 & B_{16} \\ 0 & 0 & B_{26} \\ B_{61} & B_{62} & 0 \end{bmatrix}$
$\mathbf{B}_{lt}$	Extension-Bending, Extension-Twisting and Shearing-Bending; *E-B*-*E-T*-*S-B*	$\begin{bmatrix} B_{11} & 0 & B_{16} \\ 0 & B_{22} & B_{26} \\ B_{61} & B_{62} & 0 \end{bmatrix}$
$\mathbf{B}_S$	Extension-Bending and Shearing-Twisting; *E-B*-*S-T*	$\begin{bmatrix} B_{11} & B_{12} & 0 \\ B_{21} & B_{22} & 0 \\ 0 & 0 & B_{66} \end{bmatrix}$
$\mathbf{B}_F$	Extension-Bending, Shearing-Bending, Extension-Twisting, and Shearing-Twisting; *E-B*-*S-B*-*E-T*-*S-T*	$\begin{bmatrix} B_{11} & B_{12} & B_{16} \\ B_{21} & B_{22} & B_{26} \\ B_{61} & B_{62} & B_{66} \end{bmatrix}$

*Summary of **ABD** matrix subscript notation:*
F = All elements Finite.
l = Leading diagonal elements ($B_{11} = B_{22} \neq 0$) of **B** matrix non-zero, all other elements zero.
t = Off-diagonal (or *transverse*) elements ($B_{16} = B_{26} \neq 0$) of **B** matrix non-zero, all other elements zero.
S = Simple, uncoupled form; $B_{16} = B_{26} = 0$ when applied to **B** matrix.

The fully uncoupled form ($\mathbf{A}_S\mathbf{B}_0\mathbf{D}_S$) is described as a *Simple* laminate, whereas the coupled forms are described in terms of the response that the laminate exhibits to various combination of force and moment resultants, using a *cause* and *effect* relationship. A laminate is therefore described as an *E-S* laminate if *Extension* (*E*) causes a *Shearing* (*S*) effect, whereas if *Bending* causes a *Twisting* effect then the laminate is described as a *B-T* laminate. Note that each *cause* and *effect* pair is underlined. The illustrations presented in Fig. 1 represent the thermal (contraction) response of initially flat laminates with standard ply orientations ±45, 0 and 90° in place of symbols +, –, O and ●, respectively, following a typical elevated temperature curing process. The $\mathbf{A}_S\mathbf{B}_t\mathbf{D}_S$ laminate corresponds to the extension-twisting and shearing-bending coupled configurations sought. However this laminate class is also shown to be obtained by re-aligning the principal material axis of $\mathbf{A}_S\mathbf{B}_S\mathbf{D}_S$ laminates; or $\mathbf{A}_S\mathbf{B}_{lt}\mathbf{D}_S$ for double angle-ply laminates, where the configurations now correspond to θ_1, $-\theta_1$, θ_2, $-\theta_2$ in place of the symbols +, –, O and ●. The laminate stacking sequences presented in Fig. 1 are representative examples from the minimum ply number grouping for each designation; displacement magnitudes are not to scale.

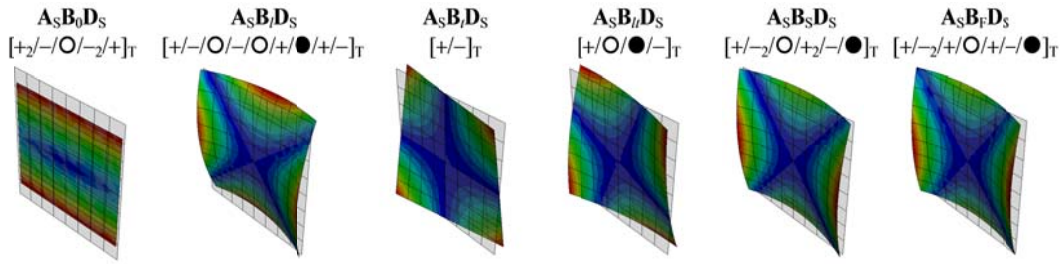

Figure 1 – Isolated coupling responses, due to free thermal contraction, for the: ($\mathbf{A_S B_0 D_S}$) *Simple* or uncoupled laminate; ($\mathbf{A_S B_t D_S}$) *B-E* laminate with bending-extension coupling; ($\mathbf{A_S B_t D_S}$) *B-S*-*T-E* laminate with bending-shearing and twisting-extension coupling; ($\mathbf{A_S B_{lt} D_S}$) *B-E*-*B-S*-*T-E* laminate with bending-extension, bending-shearing and twisting-extension coupling; ($\mathbf{A_S B_S D_S}$) *B-E*-*T-S* laminate with bending-extension and twisting-shearing coupling and; ($\mathbf{A_S B_F D_S}$) *B-E*-*B-S*-*T-E*-*T-S* or fully coupled laminate.

III. Derivation of stacking sequences

In the derivation of standard ply configurations, e.g. ±45, 0 and 90°, with bending-shearing and twisting-extension coupling, the general rules of symmetry are relaxed, i.e., neither cross plies nor angle plies are constrained to be symmetric about the laminate mid-plane. All sequences have an angle-ply (+) on one surface of the laminate, but the other surface ply may have equal (+) or opposite (–) orientation or it may indeed be a cross ply (O) of 0 or 90° orientation.

For compatibility with the previously published data[15], similar symbols have been adopted for defining all of the stacking sequences that follow. Additional symbols and parameters are necessarily included to differentiate between each orthotropic ply angle (0° and 90°), given that symmetry about the laminate mid-plane is no longer assumed. Also in common is the assumption of constant ply thickness within the laminate.

IV. Calculation of non-dimensional parameters

The calculation of the non-dimensional coupling stiffness parameters is readily demonstrated for the 8-ply laminate, designated $\mathbf{A_S B_t D_S}$ by the Engineering Science data Unit[11], with stacking sequence $[+/-_3]_A$, where elements of coupling stiffness matrix,

$$B_{ij} = \sum_{k=1}^{n} Q'_{ij}(z_k^2 - z_{k-1}^2)/2 \tag{5}$$

may be written in sequence order for the 8 individual plies, where z, representing the distance from the laminate mid-plane, is expressed here in terms of the uniform ply thickness t:

$$B_{ij} = \{Q'_{ij+}((-3t)^2 - (-4t)^2) + Q'_{ij-}((-2t)^2 - (-3t)^2) + Q'_{ij-}((-t)^2 - (-2t)^2) +$$

$$Q'_{ij-}((0)^2 - (-t)^2) + Q'_{ij+}((t)^2 - (0)^2) + Q'_{ij+}((2t)^2 - (t)^2) +$$

$$Q'_{ij+}((3t)^2 - (2t)^2) + Q'_{ij-}((4t)^2 - (3t)^2)\}/2 \tag{6}$$

where subscripts i, j = 1, 2, 6.

The coupling stiffness contribution from the angle plies is therefore:

$$B_{ij+} = 2t^2/2 \times Q'_{ij+} \tag{7}$$

$$B_{ij-} = -2t^2/2 \times Q'_{ij-} \tag{8}$$

and from the cross-plies:

$$B_{ij○} = 0 \tag{9}$$

$$B_{ij●} = 0 \tag{10}$$

These coupling stiffness terms can be written in alternative form:

$$B_{ij+} = \chi_+ t^2/4 \times Q'_{ij+} \tag{11}$$

$$B_{ij-} = \chi_- t^2/4 \times Q'_{ij-} \tag{12}$$

and

$$B_{ij○} = \chi_○ t^2/4 \times Q'_{ij○} \tag{13}$$

$$B_{ij●} = \chi_● t^2/4 \times Q'_{ij●} \tag{14}$$

respectively, where $\chi_+ = 4$, $\chi_- = -4$, $\chi_○ = 0$ and $\chi_● = 0$.

Note that $\chi_{max.} = n^2 = |\chi_+| + |\chi_-| = |\chi_○| + |\chi_●|$, which corresponds, in comparison to the above example, to $[+_4/-_4]_T$ or $[○_4/●_4]_T$ respectively. This follows a similar relationships for the extensional stiffness, where the total number of plies, $n = n_+ + n_- + n_○ + n_●$, and for the bending stiffness, where $\zeta = \zeta_+ + \zeta_- + \zeta_○ + \zeta_● = n^3$.

V. Example calculations

For a carbon-fiber/epoxy material with Young's moduli $E_1 = 161.0$GPa and $E_2 = 11.38$GPa, shear modulus $G_{12} = 5.17$GPa and Poisson's ratio $\nu_{12} = 0.38$, lamina thickness $t = 0.1397$mm and stacking sequence $[+/-_3]_A$, the non-dimensional parameters for the extensional, coupling and bending stiffness matrices are readily calculated from the geometric data presented in Table **2**, where the first two columns provide the ply number and orientation, respectively. Subsequent columns illustrate the summations, for each ply orientation, of $(z_k - z_{k-1})$, $(z_k^2 - z_{k-1}^2)/2$ and $(z_k^3 - z_{k-1}^3)/3$, relating to the **A**, **B** and **D** matrices, respectively. The distance from the laminate mid-plane, z, is expressed in term of ply thickness t, which is assumed to be of unit value.

The non-dimensional parameters arising from the summations of Table 2 are: $n_+ (= {}_A\Sigma_+) = 4$, $n_- = 4$ and $n_○ = 0$; $\chi_+ (= 2 \times {}_B\Sigma_+) = 4$, $\chi_- = -4$ and $\chi_○ = 0$ and; $\zeta_+ (= 4 \times {}_D\Sigma_+) = 256$, $\zeta_- = 256$ and $\zeta_○ = 0$, where $n^3 = 8^3 = \zeta = \zeta_+ + \zeta_- + \zeta_○ = 512$.

The extensional, coupling and bending stiffness matrix elements are:

$$A_{ij} = \{n_+ Q'_{ij+} + n_- Q'_{ij-} + n_○ Q'_{ij○}\} \times t$$

$$B_{ij} = \{\chi_+ Q'_{ij+} + \chi_- Q'_{ij-} + \chi_○ Q'_{ij○}\} \times t^2/4$$

$$D_{ij} = \{\zeta_+ Q'_{ij+} + \zeta_- Q'_{ij-} + \zeta_○ Q'_{ij○}\} \times t^3/12 \tag{15}$$

Table 2 – Calculation procedure for the non-dimensional parameters for an $\mathbf{A}_S\mathbf{B}_t\mathbf{D}_S$ laminate.

			A				**B**				**D**		
Ply k	θ	$(z_k - z_{k-1})$	${}_A\Sigma_{\circ}$	${}_A\Sigma_{-}$	${}_A\Sigma_{+}$	$(z_k^2 - z_{k-1}^2)$	${}_B\Sigma_{\circ}$	${}_B\Sigma_{-}$	${}_B\Sigma_{+}$	$(z_k^3 - z_{k-1}^3)$	${}_D\Sigma_{\circ}$	${}_D\Sigma_{-}$	${}_D\Sigma_{+}$
			0	4	4		0	-2	2		0	64	64
1	+	1		⇢	1	-7		⇢	-7	37		⇢	37
2	–	1	⇢	1		-5	⇢	-5		19	⇢	19	
3	–	1	⇢	1		-3	⇢	-3		7	⇢	7	
4	–	1	⇢	1		-1	⇢	-1		1	⇢	1	
5	+	1		⇢	1	1		⇢	1	1		⇢	1
6	+	1		⇢	1	3		⇢	3	7		⇢	7
7	+	1		⇢	1	5		⇢	5	19		⇢	19
8	–	1	⇢	1		7	⇢	7		37	⇢	37	

For fibre angles θ = ±45° and 0° in place of symbols ± and O respectively, the transformed reduced stiffnesses are given in Table 3,

Table 3 – Transformed reduced stiffness, Q'_{ij}, (N/mm^2) for carbon-fibre/epoxy with θ = -45°, 45°, 0°.

θ	Q'_{11}	Q'_{12}	Q'_{16}	Q'_{22}	Q'_{26}	Q'_{66}
-45	50,894	40,554	-37,791	50,894	-37,791	41,355
45	50,894	40,554	37,791	50,894	37,791	41,355
0	162,660	4,369	0	11,497	0	5,170

which are readily calculated from:

$$Q'_{11} = Q_{11}\cos^4\theta + 2(Q_{12} + 2Q_{66})\cos^2\theta\sin^2\theta + Q_{22}\sin^4\theta$$

$$Q'_{12} = Q'_{21} = (Q_{11} + Q_{22} - 4Q_{66})\cos^2\theta\sin^2\theta + Q_{12}(\cos^4\theta + \sin^4\theta)$$

$$Q'_{16} = Q'_{61} = \{(Q_{11} - Q_{12} - 2Q_{66})\cos^2\theta + (Q_{12} - Q_{22} + 2Q_{66})\sin^2\theta\}\cos\theta\sin\theta$$

$$Q'_{22} = Q_{11}\sin^4\theta + 2(Q_{12} + 2Q_{66})\cos^2\theta\sin^2\theta + Q_{22}\cos^4\theta$$

$$Q'_{26} = Q'_{62} = \{(Q_{11} - Q_{12} - 2Q_{66})\sin^2\theta + (Q_{12} - Q_{22} + 2Q_{66})\cos^2\theta\}\cos\theta\sin\theta$$

$$Q'_{66} = (Q_{11} + Q_{22} - 2Q_{12} - 2Q_{66})\cos^2\theta\sin^2\theta + Q_{66}(\cos^4\theta + \sin^4\theta) \qquad (16)$$

and the reduced stiffness terms are calculated from the material properties:

$$Q_{11} = E_1/(1 - \nu_{12}\nu_{21})$$

$$Q_{12} = \nu_{12}E_2/(1 - \nu_{12}\nu_{21})$$

$$Q_{22} = E_2/(1 - \nu_{12}\nu_{21})$$

$$Q_{66} = G_{12} \tag{17}$$

The final stiffness matrices for the 8-ply $[+/-_3]_A$ laminate follow from Eqs (15):

$$\begin{bmatrix} A_{11} & A_{12} & A_{16} \\ & A_{22} & A_{26} \\ \text{Sym.} & & A_{66} \end{bmatrix} = \begin{bmatrix} 56{,}879 & 45{,}323 & 0 \\ & 56{,}879 & 0 \\ \text{Sym.} & & 46{,}218 \end{bmatrix} \text{N/mm}$$

$$\begin{bmatrix} B_{11} & B_{12} & B_{16} \\ & B_{22} & B_{26} \\ \text{Sym.} & & B_{66} \end{bmatrix} = \begin{bmatrix} 0 & 0 & 1{,}475 \\ & 0 & 1{,}475 \\ \text{Sym.} & & 0 \end{bmatrix} \text{N}$$

$$\begin{bmatrix} D_{11} & D_{12} & D_{16} \\ & D_{22} & D_{26} \\ \text{Sym.} & & D_{66} \end{bmatrix} = \begin{bmatrix} 5{,}920 & 4{,}717 & 0 \\ & 5{,}920 & 0 \\ \text{Sym.} & & 4{,}811 \end{bmatrix} \text{N.mm} \tag{18}$$

These stiffness matrices represent a coupled quasi-homogeneous ($\mathbf{A}_S\mathbf{B}_t\mathbf{D}_S$) laminate, given that $D_{ij} = A_{ij}H^2/12$, possessing bending-shearing and twisting-extension coupling. By inspection, $A_{11} = A_{22}$, however, calculation reveals that $A_{66} \neq (A_{11} - A_{12})/2 = 5778$, hence the laminate does not possess in-plane (*hence out-of-plane*) isotropic properties.

VI. Lamination parameters

Lamination parameters offer an alternative set of non-dimensional expressions when ply angles are a design constraint. For (optimum) angle-ply and cross-ply laminate design, lamination parameters offer a convenient tool, since they allow the stiffness terms to be expressed as linear variables. The optimized lamination parameters may then be matched against a corresponding set of stacking sequences with given laminate thickness H ($= n \times t$). In the context of the non-dimensional parameters for uncoupled extensional (n, n_+, n_-, $n_\circ$, $n_\bullet$) and bending (ζ_+, ζ_-, $\zeta_\circ$, $\zeta_\bullet$) stiffness, only four (ξ_1, ξ_2, ξ_9 and ξ_{10}) of the twelve lamination parameters are required when the material is axis-aligned. For laminates with coupling between extensional and bending behavior, additional parameters (χ_+, χ_-, $\chi_\circ$, $\chi_\bullet$) are included to account for the coupling (**B**) matrix, and up to four additional lamination parameters must now be considered:

$$\xi_1 = \xi_1^{\,A} = \{n_+\cos(2\theta_+) + n_-\cos(2\theta_-) + n_\circ\cos(2\theta_\circ) + n_\bullet\cos(2\theta_\bullet)\}/n$$

$$\xi_2 = \xi_2^{\,A} = \{n_+\cos(4\theta_+) + n_-\cos(4\theta_-) + n_\circ\cos(4\theta_\circ) + n_\bullet\cos(4\theta_\bullet)\}/n \tag{19}$$

$$\xi_5 = \xi_1^{\,B} = \{\chi_+\cos(2\theta_+) + \chi_-\cos(2\theta_-) + \chi_\circ\cos(2\theta_\circ) + \chi_\bullet\cos(2\theta_\bullet)\}/n^2$$

$$\xi_6 = \xi_2^{\,B} = \{\chi_+\cos(4\theta_+) + \chi_-\cos(4\theta_-) + \chi_\circ\cos(4\theta_\circ) + \chi_\bullet\cos(4\theta_\bullet)\}/n^2$$

$$\xi_7 = \xi_3^{\,B} = \{\chi_+\sin(2\theta_+) + \chi_-\sin(2\theta_-) + \chi_\circ\sin(2\theta_\circ) + \chi_\bullet\sin(2\theta_\bullet)\}/n^2$$

$$\xi_8 = \xi_4^{B} = \{ \chi_{+}\sin(4\theta_{+}) + \chi_{-}\sin(4\theta_{-}) + \chi_{\circ}\sin(4\theta_{\circ}) + \chi_{\bullet}\sin(4\theta_{\bullet})\}/n^2 \quad (20)$$

Note that $\xi_8 = \xi_4^{B} = 0$ if the angle ply orientations are restricted to ±45, 0 and 90°.

$$\xi_9 = \xi_1^{D} = \{\zeta_{+}\cos(2\theta_{+}) + \zeta_{-}\cos(2\theta_{-}) + \zeta_{\circ}\cos(2\theta_{\circ}) + \zeta_{\bullet}\cos(2\theta_{\bullet})\}/n^3$$

$$\xi_{10} = \xi_2^{D} = \{\zeta_{+}\cos(4\theta_{+}) + \zeta_{-}\cos(4\theta_{-}) + \zeta_{\circ}\cos(4\theta_{\circ}) + \zeta_{\bullet}\cos(4\theta_{\bullet})\}/n^3 \quad (21)$$

Elements of the extensional (**A**), coupling (**B**) and bending (**D**) stiffness matrices are related to the lamination parameters and laminate invariants, respectively, by:

$$A_{11} = \{U_1 + \xi_1 U_2 + \xi_2 U_3\} \times H$$

$$A_{12} = A_{21} = \{-\xi_2 U_3 + U_4\} \times H$$

$$A_{22} = \{U_1 - \xi_1 U_2 + \xi_2 U_3\} \times H$$

$$A_{66} = \{-\xi_2 U_3 + U_5\} \times H \quad (22)$$

$$B_{11} = \{\xi_5 U_2 + \xi_6 U_3\} \times H^2/4$$

$$B_{12} = B_{21} = \{-\xi_6 U_3\} \times H^2/4$$

$$B_{16} = B_{61} = \{\xi_7 U_2/2 + \xi_8 U_3\} \times H^2/4$$

$$B_{22} = \{-\xi_5 U_2 + \xi_6 U_3\} \times H^2/4$$

$$B_{26} = B_{62} = \{\xi_7 U_2/2 - \xi_8 U_3\} \times H^2/4$$

$$B_{66} = \{-\xi_6 U_3\} \times H^2/4 \quad (23)$$

and

$$D_{11} = \{U_1 + \xi_9 U_2 + \xi_{10} U_3\} \times H^3/12$$

$$D_{12} = D_{21} = \{U_4 - \xi_{10} U_3\} \times H^3/12$$

$$D_{22} = \{U_1 - \xi_9 U_2 + \xi_{10} U_3\} \times H^3/12$$

$$D_{66} = \{-\xi_{10} U_3 + U_5\} \times H^3/12 \quad (24)$$

where the laminate invariants are calculated from the reduced stiffness terms Q_{ij}:

$$U_1 = \{3Q_{11} + 3Q_{22} + 2Q_{12} + 4Q_{66}\}/8$$

$$U_2 = \{Q_{11} - Q_{22}\}/2$$

$$U_3 = \{Q_{11} + Q_{22} - 2Q_{12} - 4Q_{66}\}/8$$

$$U_4 = \{Q_{11} + Q_{22} + 6Q_{12} - 4Q_{66}\}/8$$

$$U_5 = \{Q_{11} + Q_{22} - 2Q_{12} + 4Q_{66}\}/8 \tag{25}$$

VII. Equivalent Fully Isotropic Laminate

The fully isotropic laminate, or **FIL**, offers a benchmark stacking sequence configuration, against which all laminates (coupled or uncoupled) may be characterized. However, previous work[14] has shown that for thin laminates, with up to 21 plies, these so called benchmark configurations exist only for 18-ply laminates. The concept of an Equivalent **FIL**, with any number of plies, must therefore be adopted. The benchmark configuration is now replaced by a set of stiffness properties for the Equivalent **FIL**, for which no physical stacking sequence configuration exists. The stiffness properties for the Equivalent **FIL** are readily obtained from the laminate invariants, expressed in terms of their isotropic material counterparts, where $E_1 = E_2$, $\nu_{12} = \nu_{21}$, etc:

$$E_{Iso} = 2(1 + \nu_{Iso})G_{Iso} = U_1(1 - \nu_{Iso}^2) \tag{26}$$

where

$$\nu_{Iso} = U_4/U_1 \tag{27}$$

and

$$G_{Iso} = U_5 \tag{28}$$

The Young's modulus, E_{Iso}, Poisson ratio, ν_{Iso}, and shear modulus, G_{Iso}, are the equivalent isotropic material properties of a composite laminate of thickness, H, corresponding to the total number of plies, n, of uniform thickness, t, and from which the equivalent isotropic stiffness properties for laminates with any number of plies then follows:

$$A_{Iso} = A_{11} = A_{22} = E_{Iso}H/(1 - \nu_{Iso}^2) = U_1H \tag{29}$$

$$A_{12} = \nu_{Iso}A_{11} \tag{30}$$

$$A_{66} = U_5H \tag{31}$$

and the bending stiffness elements follow from:

$$D_{Iso} = E_{Iso}H^3/12(1 - \nu_{Iso}^2) = U_1H^3/12 \tag{32}$$

D_{Iso} is used in the normalization of polar plots and buckling curves that follow (Figs 3 and 5, respectively). For the same carbon-fiber/epoxy material used above, the 8-ply Equivalent **FIL** stiffness properties are readily calculated as:

$$[\mathbf{A}] = \begin{bmatrix} 120{,}280 & 39{,}162 & 0 \\ & 120{,}280 & 0 \\ \text{Sym.} & & 40{,}559 \end{bmatrix} \text{N/mm and } [\mathbf{D}] = \begin{bmatrix} 8{,}025 & 2{,}613 & 0 \\ & 8{,}025 & 0 \\ \text{Sym.} & & 2{,}706 \end{bmatrix} \text{N.mm}$$

Equivalent **FIL** stiffness properties such as these can be used to normalize the properties of other laminates. However for coupled laminates an expression for the equivalent B_{Iso} must be introduced:

$$B_{Iso} = E_{Iso}H^2/4(1 - \nu_{Iso}^2) = U_1H^2/4 \tag{33}$$

representing a value close to the maximum possible for any class of coupling behavior. For the 8-ply Equivalent **FIL** above, B_{Iso} = 21,541N, used in the normalization of the polar plots that follow (Fig. 3).

VIII. Results and Discussion

A. Stacking sequence configurations

This section presents information on the number and form of the solutions for $\mathbf{A}_S\mathbf{B}_t\mathbf{D}_S$ or *E-T-B-S* coupled laminates, which have long been thought to exist only of anti-symmetric angle-ply configurations and indeed are generally referred to as anti-symmetric laminates in the literature. However, anti-symmetric laminates have recently been shown to be prevalent in fully uncoupled[12] laminates, e.g. $[45/-45_2/45]_A$. Both groups contain balanced pairs to ensure uncoupled extensional properties; hence solutions exist only for even ply numbers. The number of stacking sequence solutions corresponding to each ply number grouping, *n*, are given in Table 4; those in parentheses indicate the number of non-symmetric stacking sequences, which exist in all ply number grouping from n = 12 plies and above, and in fact dominate the design space in the higher ply number groupings.

Table 5 presents similar data to that given in Table 4, but for stacking sequences which contain standard ply orientations, i.e., cross-plies and/or angle-ply combinations. Note that in the derivation of these laminate stacking sequences, the first (outer) ply was assumed to represent an angle-ply layer, as is common practice for damage tolerant design; thus avoiding cross-ply laminate designs. The number of subgroups from Table 5 with quasi-homogeneous orthotropic properties are highlighted in Table 6, as well as those with isotropic properties, noting that for 18-ply laminates this requires a change in the angle ply orientations from ±45, 0 and 90° to ±60 and 0° to achieve $\pi/3$ isotropy, e.g., $[60/-60_2/0_3/60_2/0/-60/60_2/-60_3/0_2/60]_T$.

Abridged listings from each of these laminate groups are presented in the appendix: Table 9 contains examples of anti-symmetric angle-ply laminates; Table 10 contains the non-symmetric counterparts and; Table 11 contains examples of the new stacking sequences with standard ply orientations.

B. Lamination parameter design spaces:

Extension-Twisting (and Shearing-Bending) coupled laminates, or *B-S-T-E* laminates, may be derived from combinations of standard ply orientations, i.e., +45, -45, 0 and 90°, and exist for all ply number groupings. The design space for laminates with up to 21 plies increase from 2,207 solutions with angle-ply configurations to 3,270,687 solutions with standard ply orientations.

Figure 2 presents the (unabridged) lamination parameter design space for (a) the Extensional and (b) Bending stiffness properties for 42,601 *B-S-T-E* laminates, representing all solutions with up to 16 plies. By contrast, Fig. 2(c) presents the concomitant laminations parameter design space for both Extension and Bending stiffness properties for 1,610 *B-S-T-E* with up to 18 plies. These are Coupled Quasi-Homogeneous Orthotropic Laminates, or QHOLs, for which the elements of the Bending stiffness matrix are derived directly from those of the Extensional stiffness matrix, i.e., $D_{ij} = A_{ij}H^2/12$. Note that the feasible domain for these lamination parameters is given by the parabola, $\xi_2 = 2\xi_1^2 - 1$, which was incorrectly stated in a previously article[19]. However, for standard ply orientations, the design space is bounded by a triangular region, as is apparent from the results in Fig. 2.

Figure 3 presents the (unabridged) three-dimensional design spaces of coupling lamination parameters, illustrated as 3rd angle orthographic projections, for quasi-homogeneous $\mathbf{A}_S\mathbf{B}_t\mathbf{D}_S$ coupled laminates; the design space is virtually identical for all $\mathbf{A}_S\mathbf{B}_t\mathbf{D}_S$ coupled laminates. The illustration of feasible domains of lamination parameters helps to provide some insight into the extent of design space for this class of coupled laminate. Note that the three-dimensional space arises by virtue of principal material axis alignment and the restriction to ±45° angle-ply

orientations, which renders $\xi_8 = 0$; off-axis material alignments and general angle-ply orientations give rise to a four-dimensional design space. The bounds on the feasible domain for coupling lamination parameters are contained within circular and Lissajous curves, where the latter is shown broken within the bounds of the design space.

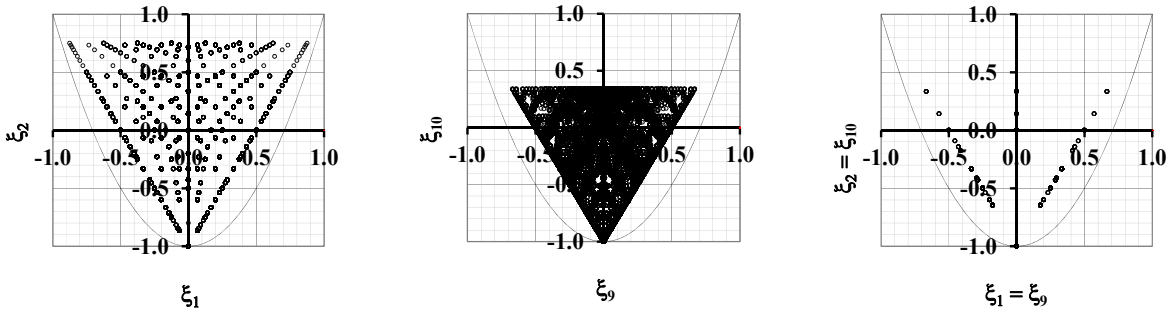

(a) (b) (c)

Figure 2 – Lamination parameter design space representing the 42,601 *B-S-T-E* laminates with bending-shearing and twisting-extension coupling ($\mathbf{A}_S\mathbf{B}_t\mathbf{D}_S$) representing all laminate with up to 16 plies for standard combinations of ply orientations, i.e., ±45, 0 and 90°, representing (a) extensional stiffness and (b) bending stiffness and (c) lamination parameters for the 1,610 *B-S-T-E* QHOLs representing all laminates with up to 18 plies.

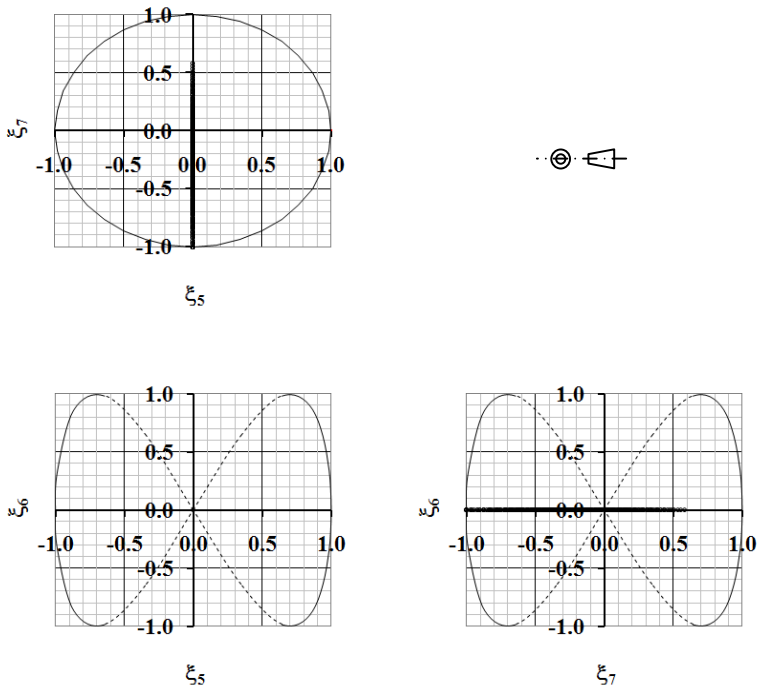

Figure 3 – Three-view illustration of the coupling lamination parameter design space for the *B-S-T-E* laminate with bending-shearing and twisting-extension coupling ($\mathbf{A}_S\mathbf{B}_t\mathbf{D}_S$) representing all laminates with up to 21 plies, with standard combinations of ply orientations, i.e., ±45, 0 and 90°. This design space is similar for QHOLs and HTCS laminates.

Table 4 – Number of $\mathbf{A_S B_t D_S}$ laminates for each ply number (n) grouping containing angle-ply orientations: ±45°. Numbers in parentheses indicate non-symmetric stacking sequences.

n	2	3	4	5	6	7	8	9	10	11	12	13	14	15	16	17	18	19	20	21
$\mathbf{A_S B_t D_S}$	1	-	2	-	4	-	7	-	16	-	35(4)	-	84(20)	-	194(70)	-	512(256)	-	1,352(850)	-

Table 5 – Number of $\mathbf{A_S B_t D_S}$ laminates for each ply number (n) grouping containing combinations of standard ply orientations: ±45°, 0° and 90°.

n	2	3	4	5	6	7	8	9	10	11	12	13	14	15	16	17	18	19	20	21
$\mathbf{A_S B_t D_S}$	1	2	4	8	16	30	63	128	256	536	1,085	2,412	4,774	11,292	21,994	58,502	111,908	329,412	632,996	2,095,268

Table 6 – Number of $\mathbf{A_S B_t D_S}$ laminates with quasi-homogeneous orthotropic properties for each ply number (n) grouping with standard ply orientations: ±45°, 0° and 90°. Numbers in parentheses indicate isotropic properties ($\mathbf{A_I B_t D_I}$); ply orientations represent ±60° and 0° for 18-ply laminates, giving π/3 isotropy.

n	2	3	4	5	6	7	8	9	10	11	12	13	14	15	16	17	18	19	20	21
$\mathbf{A_S B_t D_S}$	-	-	-	-	-	-	7	-	16	8	35	8	194	44	374(16)	162	756(110)	312	1,870	436

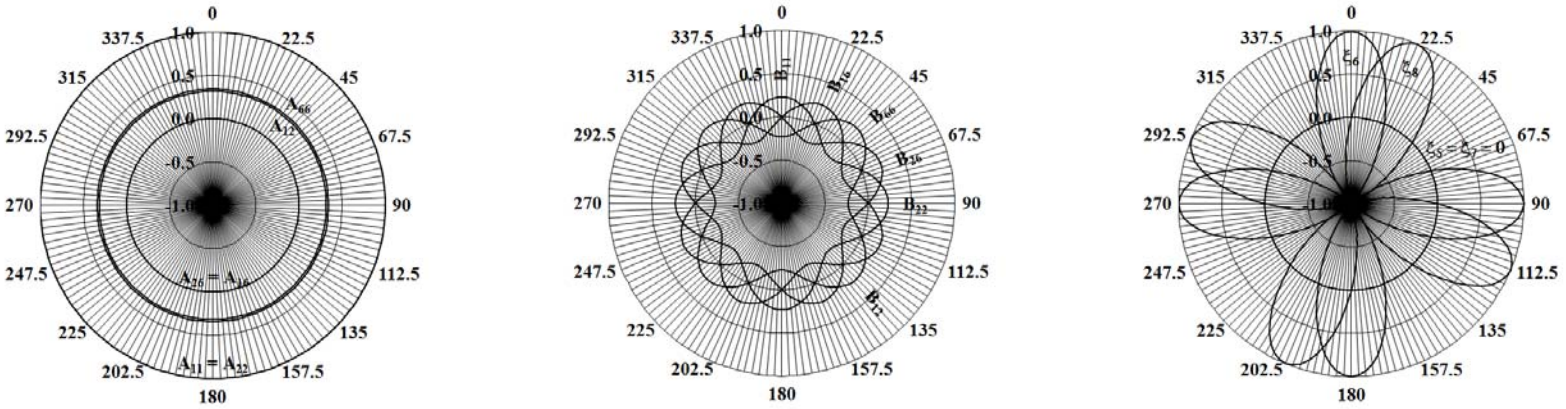

(a) $A_{ij}/A_{Iso} = D_{ij}/D_{Iso}$ (b) B_{ij}/B_{Iso} (c) ξ_5 - ξ_8

Figure 4 – Polar plots of the: (a) Isotropic **A** (and **D**) matrix elements, A_{ij}; (b) Square symmetric **B** matrix elements, B_{ij}, and; (c) Coupling lamination parameters ξ_5 - ξ_8, representing off-axis material alignment, $0 \le \beta \le 360°$, for the 16-ply hygro-thermally curvature-stable laminate stacking sequence $[+/–/–/+/–/+/+/–/O/●/●/O/●/O/O/●]_T$, with standard ply orientations ±45, 0 and 90° in place of symbols +, –, O and ●, respectively. This laminate possesses quasi-homogeneous properties, hence $D_{ij} = A_{ij}H^2/12$ and corresponds to the conditions of Table 8.

C. Hygro-thermally curvatures stable, or warp-free, sequences:

Mechanically coupled laminates with extensional isotropy have been found to provide solutions which have coupling only between Extension-Twisting (and Shearing-Bending). However they must satisfy all the lamination parameters or equivalent extensional and coupling stiffness requirements of Table 8 in order mitigate the distortions of high temperature curing; noting that $\xi_4 = \xi_8 = \xi_{12} = 0$ when standard angle plies are used, i.e., ±45, 0 and 90°, with respect to the principal material axis. Additionally for quasi-homogeneous solutions, $\xi_9 = \xi_{10} = \xi_{11} = 0$.

Eight solutions exist in laminates with up to 21 plies when standard ply angles are adopted, see Table 7. They represent $\mathbf{A_I B_S D_I}$ laminates for axis-aligned material and possess mechanical bending-extension and twisting-shearing coupling. The isotropic nature of both the extensional ($\mathbf{A_I}$) and bending ($\mathbf{D_I}$) stiffness implies that the mechanical and thermal properties are insensitive to off-axis material alignment, β. By contrast, changes in the form of the coupling stiffness matrix gives rise to an $\mathbf{A_I B_F D_I}$ laminate for general off-axis aligned material, possessing mechanical bending-extension, bending-shearing, twisting-extension and twisting-shearing coupling. $\mathbf{A_I B_S D_I}$ laminate properties occur only at 90° (π/2) intervals with respect to the principal material axis. A third class of laminate, possessing mechanical twisting-extension and bending-shearing coupling is referred to as an $\mathbf{A_I B_t D_I}$ laminate which also occurs at 90° (π/2) intervals, but off-set by 22.5° (π/8) with respect to the principal material axis. Off-axis material alignment and its effect on the laminate stiffness properties and lamination parameters for the first sequence of Table 7 can be observed in the polar plots of Fig. 4, which verifies the conditions set out in Table 8.

Table 7 – Hygro-thermally curvature-stable 16-ply quasi-homogeneous orthotropic stacking sequence configurations (*after Ref. 19.*), together with the corresponding lamination parameter, ξ_6, representing the relative coupling magnitude in $\mathbf{A_I B_S D_I}$ laminates with standard ply orientations ±45, 0 and 90° in place of symbols +, –, O and ●, respectively.

Stacking sequence	ξ_6
$[+/-/-/+/-/+/+/-/O/●/●/O/●/O/O/●]_T \equiv [+/-/-/+/-/+/+/-/●/O/O/●/O/●/●/O]_T$	1.00
$[+/-/-/+/O/●/●/O/-/+/+/-/●/O/O/●]_T \equiv [+/-/-/+/●/O/O/●/-/+/+/-/O/●/●/O]_T$	0.50
$[+/-/O/●/-/+/●/O/-/+/●/O/+/-/O/●]_T \equiv [+/-/●/O/-/+/O/●/-/+/O/●/+/-/●/O]_T$	0.25
$[+/O/-/●/-/●/+/O/-/●/+/O/+/O/-/●]_T \equiv [+/●/-/O/-/O/+/●/-/O/+/●/+/●/-/O]_T$	0.13

Table 8 – Conditions for hygro-thermally curvature-stable behavior in coupled quasi-homogeneous orthotropic laminates (*after Ref. 19.*) based on off-axis alignment of parent $\mathbf{A_I B_S D_S}$ and $\mathbf{A_I B_S D_F}$ laminate classes.

Lamination parameters and stiffness relationships with respect to material axis alignment, β.		
$\beta = m\pi/2$	$\beta = \pi/8 + m\pi/2$ ($m = 0, 1, 2, 3$)	$\beta \neq m\pi/2, \pi/8 + m\pi/2$
$(\mathbf{A_I})$		
$\begin{bmatrix} A_{11} & A_{12} & 0 \\ A_{21} & A_{11} & 0 \\ 0 & 0 & (A_{11}-A_{12})/2 \end{bmatrix}$		
$\xi_1 = \xi_2 = \xi_3 = 0$		
$(\mathbf{B_S})$	$(\mathbf{B_t})$	$(\mathbf{B_F})$
$\begin{bmatrix} B_{11} & -B_{11} & 0 \\ -B_{11} & B_{11} & 0 \\ 0 & 0 & -B_{11} \end{bmatrix}$	$\begin{bmatrix} 0 & 0 & B_{16} \\ 0 & 0 & -B_{16} \\ B_{16} & -B_{16} & 0 \end{bmatrix}$	$\begin{bmatrix} B_{11} & -B_{11} & B_{16} \\ -B_{11} & B_{11} & -B_{16} \\ B_{16} & -B_{16} & -B_{11} \end{bmatrix}$
$\xi_5 = \xi_7 = \xi_8 = 0$	$\xi_5 = \xi_6 = \xi_7 = 0$	$\xi_5 = \xi_7 = 0$

Derivatives from other parent classes of hygro-thermally curvature-stable laminates are reported elsewhere[20]. Here, attention is focused on $\mathbf{A}_I\mathbf{B}_S\mathbf{D}_F$, or *E-B-S-T*;*B-T* coupled extensionally isotropic laminates, which give rise to the coupling behavior of interest. This parent class of laminate is obtained by relaxing the orthotropic bending stiffness constraint (D_{16}, $D_{26} \neq 0$), which permits Bending-Twisting coupling in addition to Extension-Bending and Shearing-Twisting coupling. The design space contains 6, 280, 23,652 and 2,379,722 sequences with 8, 12, 16 and 20 plies, respectively. However, $\mathbf{A}_I\mathbf{B}_I\mathbf{D}_S$ laminates, achieved by off-axis alignment are limited to 6, 20, 252 and 3076 sequences, respectively; all others retain the Bending-Twisting coupling of the parent class.

D. Buckling predictions

This section presents a selection of results illustrating closed form buckling solutions, comparing bounds on previously assumed angle-ply laminates[16-18] with the new laminate listings containing combinations of angle- and cross-ply laminates. Both laminate sets possess *E-T-S-B* or Extension-Twisting and Shearing-Bending coupling. The closed form buckling solutions is given by:

$$N_x = (a/m\pi)\{T_{33} + (2T_{12}T_{23}T_{13} - T_{22}T_{13}^2 - T_{11}T_{23}^2)/(T_{11}T_{22} - T_{12}^2)\} \tag{34}$$

where

$T_{11} = A_{11}(m\pi/a)^2 + A_{66}(n\pi/b)^2$

$T_{12} = (A_{12} + A_{66})(m\pi/a)(n\pi/b)$

$T_{13} = -(3B_{16}(m\pi/a)^2 + B_{26}(n\pi/b)^2)(n\pi/b)$

$T_{22} = A_{22}(n\pi/b)^2 + A_{66}(m\pi/a)^2$

$T_{23} = -(B_{16}(m\pi/a)^2 + 3B_{26}(n\pi/b)^2)(m\pi/a)$

$T_{33} = D_{11}(m\pi/a)^4 + 2(D_{12} + 2D_{66})(m\pi/a)^2(n\pi/b)^2 + D_{22}(n\pi/b)^4$

Buckling solutions for 8-ply $\mathbf{A}_S\mathbf{B}_I\mathbf{D}_S$ laminates are presented in Figs 5(a) and (b) for stacking sequences that cannot be manufactured without specially curved tooling for laminated materials that require a high temperature curing process. Figure 5(a) presents angle-ply solutions and Fig 5(b) presents the new laminate configurations, containing cross-ply and/or angle-ply layers. The equivalent fully isotropic laminate, or FIL buckling curve is presented as a datum against which the buckling performance of the coupled laminates can be assessed. In fact the bounds on the buckling performance are only marginally improved for the by introducing combined cross-ply and angle-ply sub-sequences into the laminate design.

By contrast, the HTCS solutions all fall on or below the equivalent fully isotropic laminate, or FIL; HCTS laminates with higher ply number groupings demonstrate marginally higher buckling strength than the equivalent FIL. One of the configurations presented has been optimized[10] for maximum Extension-Twisting coupling, but this can been seen to have a negative effect on the buckling strength performance.

Natural frequency predictions are presented elsewhere[21] for this class of laminate, using a modified form of Eq. (34):

$$\omega^2 = (\pi^4/\rho)\{T_{33} + (2T_{12}T_{23}T_{13} - T_{22}T_{13}^2 - T_{11}T_{23}^2)/(T_{11}T_{22} - T_{12}^2)\} \tag{35}$$

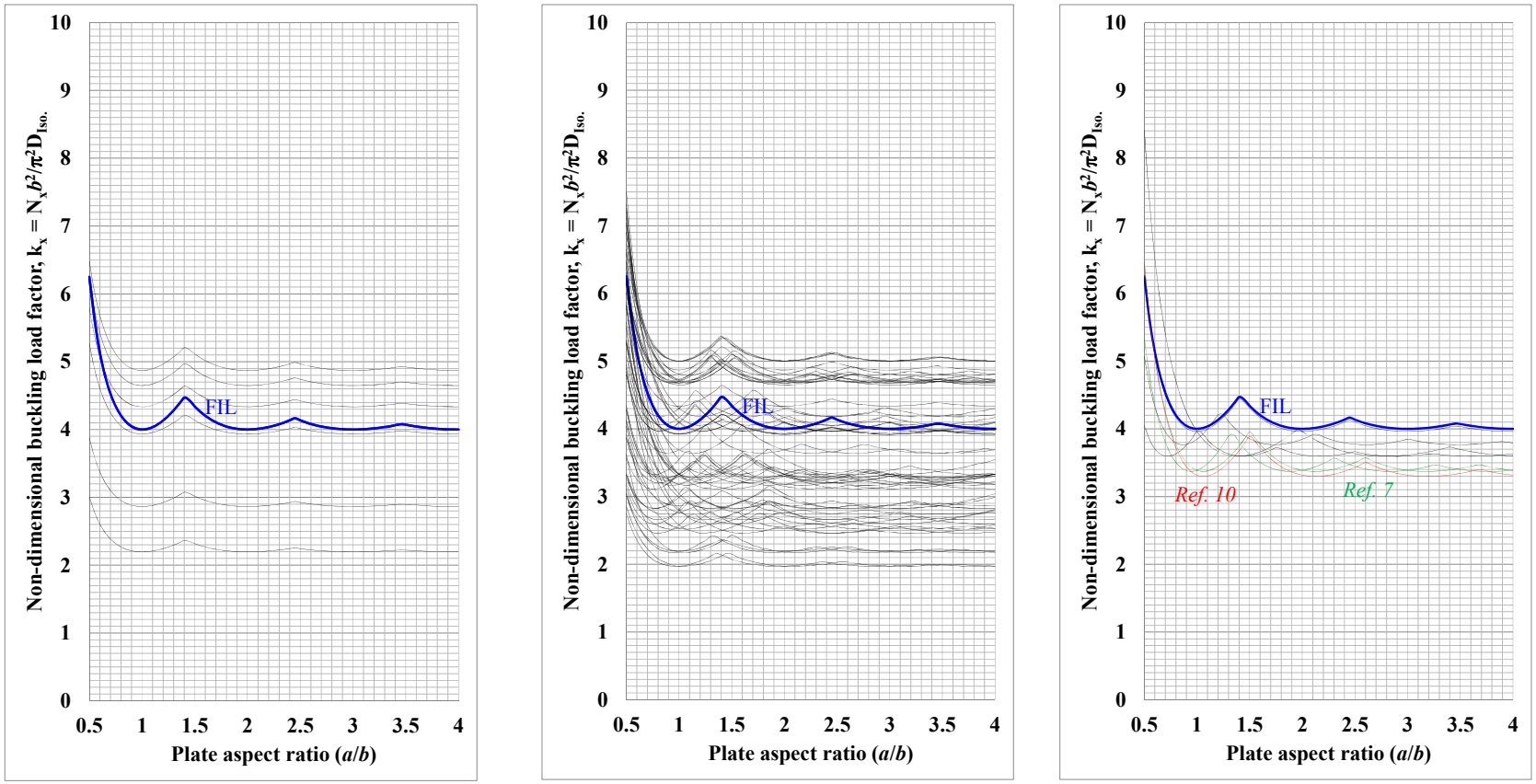

(a) (b) (c)

Figure 5 – Compression buckling curves for <u>*B*-*S*-*T*-*E*</u> coupled (a) angle-ply laminates, with orientations +45 and -45°, (b) standard laminates with ply orientations +45, -45, 0 and 90° and (c) hygro-thermally curvature-stable laminates with ply orientations +45, -45, 0 and 90° and π/8 off-axis alignment.

The buckling curves in Fig. 5(a) correspond to angle-ply laminate solutions with 8 plies: $[-45/-45/-45/-45]_A$, $[-45/-45/-45/45]_A$, $[-45/-45/45/-45]_A$, $[-45/-45/45/45]_A$, $[-45/45/-45/-45]_A$, $[-45/45/-45/45]_A$ and $[-45/45/45/45]_A$. Those in Fig. 5(b) correspond to the 63 laminate stacking sequences with standard ply orientations, i.e., combinations of +45, -45, 0 and 90° plies. Finally, those in Fig. 5(c) correspond to the HTCS solution of *Ref. 7*: $[22.5/-67.5/-67.5/22.5]_A$; new HTCS solutions: $[22.5/-67.5/-22.5/67.5]_A$, $[22.5/-22.5/-67.5/67.5]_A$, $[67.5/-67.5/-22.5/22.5]_A$, $[67.5/-22.5/-67.5/22.5]_A$, $[67.5/-22.5/-22.5/67.5]_A$; and the HTCS solution of *Ref. 10*: $[-21.5/72.1/57.9/-29.6]_A$. Together, these curves demonstrate the bounds on buckling strength for each form of laminate.

IX. Conclusions

New Extension-Twisting (and Shearing-Bending) coupled laminates have been derived from combinations of standard ply orientations, i.e., +45, -45, 0 and 90°, and have been shown to exist for all ply number groupings.

The design space for laminates with standard ply orientations has been shown to be vast in comparison to the previously assumed anti-symmetric angle ply configurations. Indeed, the design space is increased yet further with the introduction of hygro-thermally curvature-stable or HTCS laminate configurations with Extension-Twisting (and Shearing-Bending) coupled properties. This special class of laminate design is immune to thermal distortions resulting from the high temperature curing process; hence curved tooling can be avoided for such designs.

Compression buckling strength comparisons have been made between angle-ply, standard-ply and HTCS laminates using a closed form solution, for which only a relatively small increase in the bounds is apparent for the new standard ply configurations. By contrast, HTCS laminates fall on or below the buckling strength of the equivalent isotropic laminate; increasing the mechanical Extension-Twisting coupling behavior has a negative effect on the buckling strength performance.

Acknowledgements

The Royal Aeronautical Society is gratefully acknowledged for the Aerospace Speaker's Travel Award that supported the author.

References

[1]Nixon, M. W. "Extension-twist coupling of composite circular tubes with application to tilt rotor blade design," *Proc. 28th AIAA/ASME/ASCE/AHS/ASC Structures, Structural Dynamics, and Materials Conf.,* 1987, Monterey, Paper No. AIAA-87-0772.

[2]Winckler, S. J. and Hill, C. H. "Minimizing hygrothermal effects on the dimensional stability and mechanical properties of composite plates and tubes," *Proc. 8th International Conference on Composite Materials*, 1991, Honolulu.

[3]Hill, C. H. and Winckler, S. J. "The Reduction of Environmental Effects on Tension-Twist Coupled Composite Tubes," *Journal of Composite Materials*, Vol. 27, 1993, pp. 1762-1785.

[4]Baker, D. J. "Response of damaged and undamaged tailored extension-shear-coupled composite panels," *Journal of Aircraft*, Vol. 43, 2006, pp. 517-527.

[5]York, C. B. "On composite laminates with extensional-anisotropy," *Proc. 49th AIAA/ASME/ASCE/AHS/ASC Structures, Structural Dynamics, and Materials Conf.*, 2008, Schaumburg, IL, Paper No. AIAA-2008-1752.

[6]Veers, P. S., Ashwill, T. D, Sutherland, H. J., Laird, D. L., Lobitz, D. W., Griffin, D. A., Mandell, J. F., Musial, W. D., Jackson, K., Zuteck, M., Miravete, A., Tsai, S. W., Richmond, J. L. "Trends in the Design, Manufacture and Evaluation of Wind Turbine Blades," *Wind Energy*, Vol. 6, 2003, pp. 245-259.

[7]Winckler, S. J. "Hygrothermally curvature stable laminates with tension-torsion coupling," *Journal of the American Helicopter Society*, Vol. 31, 1985, pp. 56-58.

[8]Chen, H. P. "Study of hygrothermal isotropic layup and hygrothermal curvature-stable coupling composite laminates," *Proc. 44th AIAA/ASME/ASCE/AHS/ASC Structures, Structural Dynamics, and Materials Conf.*, 2003, Long beach, CA, Paper No. AIAA-2003-1506.

[9]Cross, R. J., Haynes, R. A., and Armanios, E. A. "Families of hygrothermally stable asymmetric laminated composites," *Journal of Composite Materials*, Vol. 42, 2008, pp. 697-716.

[10]Haynes, R. A. and Armanios, E. A. "New families of hygrothermally stable laminates with optimal extension-twist coupling," *AIAA Journal*, 2010, Vol. 48, No. 12, pp. 2954-2961.

[11]Engineering Sciences Data Unit, "Stiffnesses of laminated plates", ESDU Item No. 94003, 1994.

[12]York, C. B. "Characterization of non-symmetric forms of fully orthotropic laminates," *AIAA Journal of Aircraft*, Vol. 46, No. 4, 2009, pp. 1114-25.

[13]York, C. B., and Weaver, P. M. "Balanced and symmetric laminates—New perspectives on an old design rule," *Proc., 51st AIAA/ASME/ASCE/AHS/ASC Structures, Structural Dynamics, and Materials Conf.*, 2010, Orlando, FL, Paper No. AIAA-2010-2775.

[14]York C. B. "A unified approach to the characterization of coupled composite laminates: Benchmark configurations and special Cases," *Journal of Aerospace Engineering, ASCE*, Vol. 23, No. 4, 2010, pp. 1-24.

[15]Engineering Sciences Data Unit, "Laminate stacking sequences for special orthotropy (Application to fibre reinforced composites)", ESDU Item No. 82013, 1982.

[16]Whitney, J. M. "Bending-extension coupling in laminated plates under transverse loading," *Journal of Composite Materials*, Vol. 3, pp. 20-28.

[17]Leissa, A. W. "Conditions for laminated plates to remain flat under inplane loading," *Composite Structures*, Vol. 6, 1986, pp. 261-270.

[18]Qatu, M. S. and Leissa, A. W. "Buckling or transverse deflections of unsymmetrically laminated plates subjected to in-plane loads. *AIAA Journal*, Vol. 31, No. 1, 1993, pp. 189 – 194.

[19]York, C. B. "Coupled quasi-homogeneous orthotropic laminates," *Mechanics of Composite Materials*, 2011, Vol. 47, No. 4, pp. 405-426.
[20]York, C. B. "Unified approach to the characterisation of coupled composite laminates: Hygro-thermally curvature-stable configurations," *Int. J. Structural Integrity*, 2011, Vol. 2, No. 4, pp. 406-436.
[21]Li, D. and York, C. B. "Natural frequency prediction for laminated rectangular plates with extension-bending or extension-twisting and shearing-bending coupling," *Proc. I^st^ Mechanics of Nano, Micro and Macro Composite Structures Conf.*, 2012, Turin, Italy.

Appendix

Table 9 – Anti-symmetric angle-ply $\mathbf{A_S B_t D_S}$ laminates, where symbols + and –, represent +45and -45°, respectively.

Ref.	*Sequence*	n	$n_{\pm}$	$n_{\circ}$	$n_{\bullet}$	χ_{+}	χ_{-}	$\chi_{\circ}$	$\chi_{\bullet}$	ζ	$\zeta_{\pm}$	ζ_{0}	$\zeta_{\bullet}$	n_{+}	ζ_{+}
$\mathbf{A_S B_t D_S}$ 1	+ –	2	2	0	0	-2	2	0	0	4	4	0	0	1	2
$\mathbf{A_S B_t D_S}$ 2	+ + – –	4	4	0	0	-8	8	0	0	64	64	0	0	2	32
$\mathbf{A_S B_t D_S}$ 3	+ – + –	4	4	0	0	-4	4	0	0	64	64	0	0	2	32
$\mathbf{A_S B_t D_S}$ 4	+ + + – – –	6	6	0	0	-18	18	0	0	216	216	0	0	3	108
:		:													
$\mathbf{A_S B_t D_S}$ 7	+ – – + + –	6	6	0	0	-2	2	0	0	216	216	0	0	3	108
$\mathbf{A_S B_t D_S}$ 8	+ + + + – – – –	8	8	0	0	-32	32	0	0	512	512	0	0	4	256
:		:													
$\mathbf{A_S B_t D_S}$ 14	+ – – – + + + –	8	8	0	0	4	-4	0	0	512	512	0	0	4	256
$\mathbf{A_S B_t D_S}$ 15	+ + + + + – – – – –	10	10	0	0	-50	50	0	0	1000	1000	0	0	5	500
:		:													
$\mathbf{A_S B_t D_S}$ 30	+ – – – – + + + + –	10	10	0	0	14	-14	0	0	1000	1000	0	0	5	500
$\mathbf{A_S B_t D_S}$ 31	+ + + + + + – – – – – –	12	12	0	0	-72	72	0	0	1728	1728	0	0	6	864
:		:													
$\mathbf{A_S B_t D_S}$ 61	+ – – – – – + + + + + –	12	12	0	0	28	-28	0	0	1728	1728	0	0	6	864
$\mathbf{A_S B_t D_S}$ 62	+ + + + + + + – – – – – – –	14	14	0	0	-98	98	0	0	2744	2744	0	0	7	1372
:		:													
$\mathbf{A_S B_t D_S}$ 125	+ – – – – – – + + + + + + –	14	14	0	0	46	-46	0	0	2744	2744	0	0	7	1372
$\mathbf{A_S B_t D_S}$ 126	+ + + + + + + + – – – – – – – –	16	16	0	0	-128	128	0	0	4096	4096	0	0	8	2048
:		:													
$\mathbf{A_S B_t D_S}$ 249	+ – – – – – – – + + + + + + + –	16	16	0	0	68	-68	0	0	4096	4096	0	0	8	2048
$\mathbf{A_S B_t D_S}$ 250	+ + + + + + + + + – – – – – – – – –	18	18	0	0	-162	162	0	0	5832	5832	0	0	9	2916
:		:													
$\mathbf{A_S B_t D_S}$ 505	+ – – – – – – – + + + + + + + + –	18	18	0	0	94	-94	0	0	5832	5832	0	0	9	2916
$\mathbf{A_S B_t D_S}$ 506	+ + + + + + + + + + – – – – – – – – – –	20	20	0	0	-200	200	0	0	8000	8000	0	0	10	4000
:		:													
$\mathbf{A_S B_t D_S}$ 1007	+ – – – – – – – – – + + + + + + + + + –	20	20	0	0	124	-124	0	0	8000	8000	0	0	10	4000

Table 10 – Non-symmetric angle-ply $\mathbf{A_S B_t D_S}$ laminates, where symbols + and −, represent +45and -45°, respectively.

Ref.	*Sequence*	n	$n_{\pm}$	$n_{\circ}$	$n_{\bullet}$	χ_{+}	χ_{-}	$\chi_{\circ}$	$\chi_{\bullet}$	ζ	$\zeta_{\pm}$	ζ_{0}	$\zeta_{\bullet}$	n_{+}	ζ_{+}
$\mathbf{A_S B_t D_S}$ 1	+ − − + + + − + − − − +	12	12	0	0	-12	12	0	0	1728	1728	0	0	6	864
:		:													
$\mathbf{A_S B_t D_S}$ 4	+ − − − + − + + + − − +	12	12	0	0	12	-12	0	0	1728	1728	0	0	6	864
$\mathbf{A_S B_t D_S}$ 5	+ − + + + − + − − − + + − −	14	14	0	0	-38	38	0	0	2744	2744	0	0	7	1372
:		:													
$\mathbf{A_S B_t D_S}$ 24	+ − − − − − + + + + − + − +	14	14	0	0	34	-34	0	0	2744	2744	0	0	7	1372
$\mathbf{A_S B_t D_S}$ 25	+ + − + + + − + − − − + + − − −	16	16	0	0	-68	68	0	0	4096	4096	0	0	8	2048
:		:													
$\mathbf{A_S B_t D_S}$ 94	+ − − − − + − − + + + + − + − +	16	16	0	0	44	-44	0	0	4096	4096	0	0	8	2048
$\mathbf{A_S B_t D_S}$ 95	+ + + − + + + − + − − − + + − − − −	18	18	0	0	-102	102	0	0	5832	5832	0	0	9	2916
:		:													
$\mathbf{A_S B_t D_S}$ 350	+ − − − − − − − + + + + + + − − + +	18	18	0	0	78	-78	0	0	5832	5832	0	0	9	2916
$\mathbf{A_S B_t D_S}$ 351	+ + + + − + + + − + − − − + + − − − − −	20	20	0	0	-140	140	0	0	8000	8000	0	0	10	4000
:		:													
$\mathbf{A_S B_t D_S}$ 1200	+ − − − − − − − + − + + + + − + + + − +	20	20	0	0	104	-104	0	0	8000	8000	0	0	10	4000

Table 11 – $\mathbf{A_S B_t D_S}$ laminates for standard ply orientations, where symbols +, –, ○ and ●, represent +45, -45, 0 and 90°, respectively.

Ref.	*Sequence*	n	$n_{\pm}$	$n_{\circ}$	$n_{\bullet}$	χ_{+}	χ_{-}	$\chi_{\circ}$	$\chi_{\bullet}$	ζ	$\zeta_{\pm}$	ζ_{0}	$\zeta_{\bullet}$	n_{+}	ζ_{+}
$\mathbf{A_S B_t D_S}$ *1*	+ +	2	2	0	0	**-2**	**2**	**0**	**0**	8	8	0	0	1	4
$\mathbf{A_S B_t D_S}$ *2*	+ ● –	3	2	0	1	-4	4	0	0	27	26	0	1	1	13
$\mathbf{A_S B_t D_S}$ *3*	+ ○ –	3	2	1	0	-4	4	0	0	27	26	1	0	1	13
$\mathbf{A_S B_t D_S}$ *4*	+ ● ● –	4	2	0	2	-6	6	0	0	64	56	0	8	1	28
:		:													
$\mathbf{A_S B_t D_S}$ *7*	+ – + –	4	4	0	0	**-4**	**4**	**0**	**0**	64	64	0	0	2	32
$\mathbf{A_S B_t D_S}$ *8*	+ ● ● ● –	5	2	0	3	**-8**	**8**	**0**	**0**	125	98	0	27	1	49
:		:													
$\mathbf{A_S B_t D_S}$ *15*	+ – ○ + –	5	4	1	0	**-4**	**4**	**0**	**0**	125	124	1	0	2	62
$\mathbf{A_S B_t D_S}$ *16*	+ ● ● ● ● –	6	2	0	4	**-10**	**10**	**0**	**0**	216	152	0	64	1	76
:		:													
$\mathbf{A_S B_t D_S}$ *31*	+ – – + + –	6	6	0	0	**-2**	**2**	**0**	**0**	216	216	0	0	3	108
$\mathbf{A_S B_t D_S}$ *32*	+ ● ● ● ● –	7	2	0	5	**-12**	**12**	**0**	**0**	343	218	0	125	1	109
:		:													
$\mathbf{A_S B_t D_S}$ *61*	+ – + ○ – + –	7	6	1	0	**-8**	**8**	**0**	**0**	343	342	1	0	3	171
$\mathbf{A_S B_t D_S}$ *62*	+ ● ● ● ● ● ● –	8	2	0	6	**-14**	**14**	**0**	**0**	512	296	0	216	1	148
:		:													
$\mathbf{A_S B_t D_S}$ *124*	+ – – – + + + –	8	8	0	0	**4**	**-4**	**0**	**0**	512	512	0	0	4	256
$\mathbf{A_S B_t D_S}$ *125*	+ ● ● ● ● ● ● ● –	9	2	0	7	**-16**	**16**	**0**	**0**	729	386	0	343	1	207
:		:													
$\mathbf{A_S B_t D_S}$ *252*	+ – – – ○ + + + –	9	8	1	0	**8**	**-8**	**0**	**0**	729	728	1	0	4	207
$\mathbf{A_S B_t D_S}$ *253*	+ ● ● ● ● ● ● ● ● –	10	2	0	8	**-18**	**18**	**0**	**0**	1000	488	0	512	1	324
:		:													
$\mathbf{A_S B_t D_S}$ *508*	+ – – – – + + + + –	10	10	0	0	**14**	**-14**	**0**	**0**	1000	1000	0	0	5	252
$\mathbf{A_S B_t D_S}$ *509*	+ ● ● ● ● ● ● ● ● ● –	11	2	0	9	**-20**	**20**	**0**	**0**	1331	602	0	729	1	436
:		:													
$\mathbf{A_S B_t D_S}$ *1044*	+ – – – – ○ + + + + –	11	10	1	0	**20**	**-20**	**0**	**0**	1331	1330	1	0	5	412
$\mathbf{A_S B_t D_S}$ *1045*	+ ● ● ● ● ● ● ● ● ● –	12	2	0	10	**-22**	**22**	**0**	**0**	1728	728	0	1000	1	788
:		:													
$\mathbf{A_S B_t D_S}$ *2129*	+ – – – – – + + + + + –	12	12	0	0	**28**	**-28**	**0**	**0**	1728	1728	0	0	6	544
$\mathbf{A_S B_t D_S}$ *2130*	+ ● ● ● ● ● ● ● ● ● ● ● –	13	2	0	11	**-24**	**24**	**0**	**0**	2197	866	0	1331	1	495
:		:													
$\mathbf{A_S B_t D_S}$ *4541*	+ – – – – – ○ + + + + + –	13	12	1	0	**36**	**-36**	**0**	**0**	2197	2196	1	0	6	761
:		:													

Table 12 – $\mathbf{A_S B_t D_S}$ quasi-homogeneous laminates (*after Ref. 19.*)

Ref.	*Sequence*	n	$n_{\pm}$	$n_{\circ}$	$n_{\bullet}$	χ_{+}	χ_{-}	$\chi_{\circ}$	$\chi_{\bullet}$	ζ	$\zeta_{\pm}$	ζ_0	$\zeta_{\bullet}$	n_{+}	ζ_{+}
$\mathbf{A_S B_t D_S}$ 1	– +	2	2	0	0	-2	2	0	0	8	8	0	0	1	4
$\mathbf{A_S B_t D_S}$ 2	– – + +	4	4	0	0	-8	8	0	0	64	64	0	0	2	32
$\mathbf{A_S B_t D_S}$ 3	– + – +	4	4	0	0	-4	4	0	0	64	64	0	0	2	32
$\mathbf{A_S B_t D_S}$ 4	– – – + + +	6	6	0	0	-18	18	0	0	216	216	0	0	3	108
:		:													
$\mathbf{A_S B_t D_S}$ 7	– + + – – +	6	6	0	0	-2	2	0	0	216	216	0	0	3	108
$\mathbf{A_S B_t D_S}$ 9	– – – – + + + +	8	8	0	0	-32	32	0	0	512	512	0	0	4	256
:		:													
$\mathbf{A_S B_t D_S}$ 14	– + + + – – – +	8	8	0	0	4	-4	0	0	512	512	0	0	4	256
$\mathbf{A_S B_t D_S}$ 15	– – – – – + + + + +	10	10	0	0	-50	50	0	0	1000	1000	0	0	5	500
:		:													
$\mathbf{A_S B_t D_S}$ 30	– + + + + – – – – +	10	10	0	0	14	-14	0	0	1000	1000	0	0	5	500
$\mathbf{A_S B_t D_S}$ 31	– ● ● – – ● + + ● ● +	11	6	0	5	-32	32	0	0	1331	726	0	605	3	363
:		:													
$\mathbf{A_S B_t D_S}$ 38	– ○ ○ + + ○ – – ○ ○ +	11	6	5	0	-8	8	0	0	1331	726	605	0	3	363
$\mathbf{A_S B_t D_S}$ 39	– – – – – – + + + + + +	12	12	0	0	-72	72	0	0	1728	1728	0	0	6	864
:		:													
$\mathbf{A_S B_t D_S}$ 73	– + + + + + – – – – – +	12	12	0	0	28	-28	0	0	1728	1728	0	0	6	864
$\mathbf{A_S B_t D_S}$ 74	– – ● + – ● + – – + + ● +	13	10	0	3	-40	40	0	0	2197	1690	0	507	5	845
:		:													
$\mathbf{A_S B_t D_S}$ 81	– + ○ – + ○ – + – – ○ +	13	10	3	0	-8	8	0	0	2197	1690	507	0	5	845
$\mathbf{A_S B_t D_S}$ 82	– ● ● ● – ● – + ● + ● ● ● +	14	6	0	8	-38	38	0	0	2744	1176	0	1568	3	588
:		:													
$\mathbf{A_S B_t D_S}$ 275	– + + + + + + – – – – – – +	14	14	0	0	46	-46	0	0	2744	2744	0	0	7	1372
$\mathbf{A_S B_t D_S}$ 276	– – – ● + ● – – – + + + + ● +	15	12	0	3	-72	72	0	0	3375	2700	0	675	6	1350
:		:													
$\mathbf{A_S B_t D_S}$ 319	– + + ○ + ○ + – – – + + ○ –	15	12	3	0	24	-24	0	0	3375	2700	675	0	6	1350
$\mathbf{A_S B_t D_S}$ 320	– ● ● – ● – – ● ● + + ● + ● ● +	16	8	0	8	-64	64	0	0	4096	2048	0	2048	4	1024
:		:													
$\mathbf{A_S B_t D_S}$ 693	– + + + + + + + – – – – – – – +	16	16	0	0	68	-68	0	0	4096	4096	0	0	8	2048
$\mathbf{A_S B_t D_S}$ 694	– ● – ● – ● – + – ● ● + ● + + + ●	17	10	0	7	-80	80	0	0	4913	2890	0	2023	5	1445
:															
$\mathbf{A_S B_t D_S}$ 855	– + ○ + + + + + ○ – – – – – ○ – +	17	14	3	0	56	-56	0	0	4913	4046	867	0	7	2023
$\mathbf{A_S B_t D_S}$ 856	– ● ● ● ● ● – – ● ● + + ● ● ● ● ● +	18	6	0	12	-50	50	0	0	5832	1944	0	3888	3	972
:		:													